RESTRICTED INVESTIGATION REPORT 1693R

CSIRO

INSTITUTE OF ENERGY AND EARTH RESOURCES

DIVISION OF MINERAL PHYSICS AND MINERALOGY

THEORETICAL ROCK MAGNETISM OF MONOCLINIC PYRRHOTITE

(AMIRA PROJECT P78/96B - APPLICATIONS OF ROCK MAGNETISM

D.A. CLARK

P.O. Box 136
NORTH RYDE 2113
AUSTRALIA

MAY 1987

DISTRIBUTION LIST

CSIRO Division of Mineral Physics and Mineralogy	Copy no.
D. Clark	1
P. Schmidt	2
B. Embleton	3
Records	4
AMIRA	5-22

This is copy no.....of 22

TABLE OF CONTENTS

LIST OF TABLES*

LIST OF FIGURES

* Table and Figures no.s marked with an asterisk in the text refer to CSIRO Restricted Investigation Report 1411R, "Hysteresis Properties of Sized Dispersed Monoclinic Pyrrhotite Grains," D.A. Clark (April, 1983).

1 Magnetic hysteresis parameters of MD grains

Figure 4.1a depicts the intrinsic hysteresis loop for a MD pyrrhotite grain for the case where the applied field is parallel to the basal plane of the crystal.

The internal field H_i is related to the external (applied) field H_e by

$$H_i = H_e - NJ \qquad 1)$$

where J is the magnetisation and N is, by definition, the self-demagnetising factor of the grain.

From eq. 1 it follows that H_e corresponding to a point (J,H_i) on the intrinsic hysteresis loop can be found by constructing a line of slope $-1/N$ from (J,H_i) to the horizontal axis (Néel, 1955). In this way we can obtain the external hysteresis loop $(J\text{-}H_e)$ from the intrinsic $(J\text{-}H_i)$ loop.

Consider an initially demagnetised grain subjected to a saturating field in the forward direction which is then reduced to zero. The grain is then at the point $(J_{rs},-H_{iR})$ on the intrinsic hysteresis loop, where J_{rs} is the saturation remanence.

As $H_e = 0$, we have from 1)

$$-H_{iR} = - NJ_{rs}$$

$$\therefore \quad J_{rs} = H_{iR}/N \qquad 2)$$

We now assume the intrinsic hysteresis loop is linear in the region about the coercive force point $(0,-H_c)$, with slope S.

Therefore from Fig. 1a

$$J_{rs}/[-H_{iR} - (-H_c)] = J_{rs}/[H_c - H_{iR}] = S$$

Using 2) we have

$$J_{rs} = S(H_c - NJ_{rs})$$

Solving for J_{rs}

$$J_{rs} = H_c/(N + 1/S) \qquad 3)$$

As $S \to \infty$, $J_{rs} \to H_c/N$, which is the relationship derived by Néel (1955) and Stacey and Banerjee (1974). As pointed out by Smith and Merrill (1982) neglect of the finite slope of the sides of the hysteresis loop invalidates empirical estimates of N. Only if $S >> 1/N$ will N be reliably estimated by H_c/J_{rs}, but this condition cannot be justified *a priori*.

The potential energy of a domain wall in a crystal is a function of wall position due to interactions with defects such as dislocations and non-magnetic inclusions. In the absence of magnetostatic forces, therefore, domain walls will reside in local potential energy minima, which we will call intrinsic energy minima. Within potential energy wells the domain walls are reversibly displaced from the intrinsic minima due to the internal field H_i. For small wall displacements the induced magnetisation is linear in H_i and is equal to $\chi_i H_i$, where χ_i is the intrinsic susceptibility (see Fig. 1b).

As a grain is taken around a hysteresis loop, domain walls are irreversibly displaced from their original positions to new potential wells. Denote the change in magnetisation associated with displacement of walls from original positions to new intrinsic minima by J_{irr}. Due to the internal field the walls are reversibly displaced from the intrinsic minima, and we assume linearity of this induced magnetisation in H_i.

Therefore the total magnetisation, J, of the grain is given by

$$J = \chi_i H_i + J_{irr} \qquad 4)$$

But $$H_i = H_e - NJ = H_e - N\chi_i H_i - NJ_{irr}$$

$$\therefore \quad H_i = (H_e - NJ_{irr})/(1+N\chi_i) \qquad 5)$$

By definition when $H_e = 0$, $J = J_r$ (the observed remanence of the grain).

Therefore, when $H_e = 0$,

$$H_i = -NJ_r = -NJ_{irr}/(1 + N\chi_i)$$

$$\therefore \quad J_r = J_{irr}/(1 + N\chi_i) \qquad 6)$$

Substituting (4.6) into (4.5)

$$H_i = H_e/(1 + N\chi_i) - NJ_r \qquad 7)$$

This is equivalent to eq. 10.2 of Stacey and Banerjee (1974, p.139).

Denote the observed susceptibility by χ_o. By definition the induced magnetisation is $\chi_o H_e$ and the total magnetisation $J = \chi_o H_e + J_r$.

From 4)

$$J = \chi_o H_e + J_r = \chi_i H_i + J_{irr}$$

Using 6), we have

$$\chi_o H_e + J_r = \chi_i H_i + J_r(1 + N\chi_i)$$

$$\therefore \quad \chi_o H_e = \chi_i H_i + N\chi_i J_r = \chi_i(H_i + NJ_r)$$

7) gives

$$H_i + NJ_r = H_e/(1 + N\chi_i)$$

$$\therefore \quad \chi_o = \chi_i/(1 + N\chi_i) \qquad 8)$$

Solving 8) for χ_i

$$\chi_i = \chi_o/(1 - N\chi_o) \qquad 9)$$

Also

$$(1 + N\chi_i) = \chi_i/\chi_o = 1/(1 - N\chi_o) \qquad 10)$$

We now consider the relationship between coercivity of remanence H_{cr} and coercive force H_c. Let the point on the intrinsic hysteresis loop from which the grain returns to the demagnetised state upon removal of the applied field be $(-J_D,-H_{iD})$. Clearly the corresponding external field is $-H_{cr}$.

From 1)

$$-H_{cr} = -H_{iD} + N(-J_D)$$

$$\therefore \quad H_{cr} = H_{iD} + NJ_D$$

The slope of the J-H_i curve through the origin is (approximately) χ_i.

$$\therefore \quad J_D = \chi_i H_{iD}$$

It follows that

$$H_{cr} = (1 + N\chi_i)H_{iD} \qquad 11)$$

From Fig. 1,

$$S = J_D/(H_{iD} - H_c) = \chi_i H_{iD}/(H_{iD} - H_c)$$

$$\therefore \quad H_{iD} = H_c/(1 - \chi_i/S) \qquad 12)$$

Substituting 12) into 11)

$$H_{cr} = (1 + N\chi_i)\, H_c/(1 - \chi_i/S) \qquad 13)$$

As $S \to \infty$, $H_{cr} \to (1 + N\chi_i)H_c$, which is the relationship given by Stacey and Banerjee (1974, p.82).

Substituting 9) into 13) we can relate N and S to the observable quantities H_{cr}, H_c and χ_o

$$H_{cr} = H_c/[1 - \chi_o(N + 1/S)] \qquad 14)$$

Although in 3) and 14) we have two equations involving the unknowns N and S, they are not independent and therefore cannot be solved for N and S. However the model can be checked experimentally for self-consistency by testing the following relationships, derived from 3) and 14)

$$H_{cr} = J_{rs}H_c/(J_{rs} - \chi_o H_c) \qquad 15)$$

It is apparent from the above discussion that empirical determination of N and S requires additional information. This information can be conveniently obtained from alternating field demagnetisation, or from IRM acquisition curves.

First let us consider AF demagnetisation of saturation remanence. The peak alternating field required to demagnetise half the saturation remanence is known as the median destructive field (mdf) of SIRM, and is denoted by $H_{\frac{1}{2}}$.

Let J_r' be the residual remanence after demagnetisation in a peak alternating field H_e. From 7), as the field alternates between $\pm H_e$, the internal field of the grains varies between the limits

$$-H_e/(1 + N\chi_i) - NJ_r' \leq H_i \leq H_e/(1 + N\chi_i) - NJ_r' \qquad 16)$$

The magnitude of the internal field acting to demagnetise the grain is therefore $|-H_e/(1 + N\chi_i) - J_r'| = H_e/(1 + N\chi_i) + NJ_r'$. The internal field corresponding to $H_e = H_{\frac{1}{2}}$ is H_{iD}. Whereas a DC back-field reverses 50% of the original remanence, thereby cancelling the residual remanence, an alternating internal field equal to H_{iD} randomises 50% of the remanence, leaving a

residual remanence of $J_{rs}/2$.

We have therefore

$$H_{\frac{1}{2}}/(1 + N\chi_i) + NJ_{rs}/2 = H_{iD}$$

$$\therefore \quad H_{\frac{1}{2}} = (1 + N\chi_i)\ (H_{iD} - NJ_{rs}/2)$$

Using 10) and 11)

$$H_{\frac{1}{2}} = H_{cr} - NJ_{rs}/2(1 - N\chi_o) \qquad 17)$$

The mdf of SIRM is therefore always less than the coercivity of remanence. The self-demagnetising factor N can be expressed in terms of measurable parameters as

$$N = 2(H_{cr} - H_{\frac{1}{2}})/\left[J_{rs} + 2\chi_o(H_{cr} - H_{\frac{1}{2}})\right] \qquad 18)$$

The coercivity of remanence acquisition H'_{cr} is defined as the external field required to produce IRM equal to $0.5J_{rs}$ in an initially demagnetised specimen. During initial IRM acquisition the applied field is opposed by the self-demagnetising fields of the grains, whereas DC demagnetisation is assisted by the self-demagnetising fields. Thus we expect IRM acquisition to be more difficult than DC demagnetisation, and consequently H'_{cr} should be greater than H_{cr}.

To calculate H'_{cr} we assume that the internal field required to irreversibly displace domain walls from their equilibrium positions in the demagnetised state ($J_r = 0$, $H_e = 0$), such that J_r after removal of the applied field is $0.5\ J_{rs}$, is equal to the internal field which can reverse half the saturation remanence. This is reasonable if the heights of potential energy barriers separating stable positions of domain walls are uncorrelated with the wall positions (and hence with the

magnetisation state). Whilst this probably does not apply to individual grains, particularly if the crystal defects are ordered, it should be true on average for an assemblage of grains.

Alternatively we may consider the approximation that the effective field acting on grains with domains separated by 180^{o} walls is the field component parallel to the domain magnetisation. This premise is reasonable for applied fields insufficient to remove domain structure (i.e. within the region of magnetisation by domain wall displacement). Then, for a randomly oriented assemblage of identical grains the internal field required to reverse 50% of domain magnetisations will be independent of the initial magnetisation state. This argument follows from the principles discussed by Chikazumi and Charap (1978, Ch. 12).

We therefore have, from 7)

$$H_{iD} = H'_{cr}/(1 + N\chi_i) - NJ_{rs}/2$$

$$\therefore \quad H'_{cr} = (1 + N\chi_i)(H_{iD} + NJ_{rs}/2)$$

from which we obtain, using 10) and 11)

$$H'_{cr} = H_{cr} + NJ_{rs}/2(1 - N\chi_o) \qquad 19)$$

From 17) and 19)

$$H'_{cr} - H_{cr} = NJ_{rs}/2(1 - N\chi_o) = H_{cr} - H_{\frac{1}{2}} \qquad 20)$$

$$\therefore \quad H'_{cr} + H_{\frac{1}{2}} = 2H_{cr} \qquad 21)$$

Eq. 21 is a theoretically derived relationship which is empirically supported by the data of Dankers (1981) for dispersed haematite, magnetite and titanomagnetite powders. The relationship automatically holds for non-interacting SD

grains as $H'_{cr} \simeq H_{cr} \simeq H_{\frac{1}{2}}$ for this case (Wohlfarth, 1958). Thus eq. 21 should be approximately satisfied for grains ranging from SD to large MD sizes.

The relationships between observable hysteresis properties and the fundamental parameters N and S given by 3), 8), 14), 15), and 17 - 20) are derived assuming the applied field is parallel or antiparallel to the domain magnetisations. In the case of MD titanomagnetites the above relationships should apply quite closely as the domain magnetisations tend to be aligned by the applied field and the hysteresis properties are dominated by domains which are approximately aligned with the applied field. For example, the saturation remanence for a randomly oriented assemblage of magnetite grains will be 0.87 of the value for an assemblage of grains with domains aligned parallel to the field (Chikazumi and Charap, 1978, p.251).

However, the relationships between hysteresis parameters will be significantly modified for a randomly oriented assemblage of pyrrhotite grains as the magnetisation in fields less than ~20kG will be essentially confined to the basal plane.

We will denote the hysteresis properties of a randomly oriented assemblage by $\bar{J}_{rs}$, $\bar{H}_c$ etc. Let θ be the angle between the $[00\bar{1}]$ axis and the applied field $\tilde{H}$. The self-demagnetising factor in the basal plane is N and is assumed to be isotropic.

In the basal plane $\chi_o = \chi_i/(1 + N\chi_i)$. The observed susceptibility of a grain at angle θ to the field is $\chi_o(\theta) = \chi_o \sin^2\theta$. The susceptibility of the assemblage is

therefore

$$\bar{\chi}_o = \chi_o \overline{\sin^2\theta} = \int_o^{\pi/2} \chi_o \sin^2\theta . \sin\theta \, d\theta = 2\chi_o/3 \qquad 22)$$

where we have integrated over a hemisphere. We have neglected the contribution of susceptibility along $[\bar{0}01]$ as this is two orders of magnitude smaller than χ_i

$$\therefore \quad \bar{\chi}_o = 2\chi_i/3(1 + N\chi_i) \qquad 23)$$

To calculate the saturation remanence we neglect undersaturation of the small fraction of grains with $[\bar{0}01]$ axes lying in a narrow cone about $\tilde{H}$. The component of remanence parallel to H of a grain at angle θ is then $J_{rs}\sin\theta$.

$$\therefore \quad \bar{J}_{rs} = J_{rs}\overline{\sin\theta} = J_{rs} \int_o^{\pi/2} \sin^2\theta \, d\theta$$

$$\therefore \quad \bar{J}_{rs} = \pi J_{rs}/4 \qquad 24)$$

The maximum error due to undersaturation of grains which have basal planes nearly perpendicular to $\tilde{H}$ can be estimated as follows.

All grains with $\theta > \theta_o = \sin^{-1}(H_{sat}/H)$ will be saturated, where H_{sat} is the saturating field within the basal plane. The remanence attributed to these undersaturated grains in the above integration is $\int_o^{\theta_o} J_{rs} \sin^2\theta \, d\theta = J_{rs}(\theta_o - \sin\theta_o\cos\theta_o)/2$. The error in $\bar{J}_{rs}$ is less than this. For example $H = 2H_{sat}$ gives an upper limit to the error of 6%. $H = 3H_{sat}$ gives an error of less than 2%.

In order to calculate the coercivity parameters of a randomly oriented assemblage of non-interacting grains we invoke the principle that the observed external hysteresis loop is the superposition of the external hysteresis loops of

individual grains or, in other words, the external hysteresis loops of a grain at angle θ, integrated over all orientations.

Because only the component of $\tilde{H}$ in the basal plane is effective in taking a grain around its hysteresis loop, the coercive force of a grain at angle θ is given by $H_c(\theta) = H_c/\sin\theta$, provided the grain has first been saturated in the forward direction (Fig. 2a). Since $H_c(\theta) > H_c$ the coercive force of the assemblage will be greater than H_c, the basal plane coercive force. Although the grains with basal planes almost perpendicular to $\tilde{H}$ will be undersaturated (for instance as $\theta \to o$, $H_c(\theta)$ approaches zero - not infinity as would be predicted from the formula $H_c/\sin\theta$), the contribution of these grains to the magnetisation is negligible, as was seen above.

Following saturation of the assemblage in the forward direction the reverse field which reduces $\bar{J}$ to zero is by definition $H = -\bar{H}_c$. Define θ_1 by $H_c(\theta_1) = \bar{H}_c$. Thus $J(\theta_1) = 0$ when $H = -H_c(\theta_1) = -\bar{H}_c$.

The slope of the intrinsic hysteresis loop in the vicinity of the coercive force point is S.

$$\therefore \quad J(\theta) \simeq S\left[\bar{H}_i(\theta) - H_i(\theta_1)\right] \quad (\text{when } H = -\bar{H}_c)$$

$$= S\left[(-\bar{H}_c\sin\theta - NJ(\theta)) - (-\bar{H}_c\sin\theta_1)\right]$$

$$\therefore \quad J(\theta) = S\bar{H}_c\left[\sin\theta_1 - \sin\theta\right] - NS\,J(\theta)$$

Solving for $J(\theta)$: $J(\theta) = S\bar{H}_c\left[\sin\theta_1 - \sin\theta\right]/(1 + NS)$ 25)

Integrating over all orientations

$$\bar{J} = \overline{J(\theta)\sin\theta} = \left[S\bar{H}_c/(1 + NS)\right]\int_0^{\pi/2}(\sin\theta_1 - \sin\theta)\sin^2\theta\,d\theta$$

$$= S\bar{H}_c\left[\pi\sin\theta_1/4 - 2/3\right]/(1 + NS)$$

The condition $\bar{J} = 0$ gives $\sin\theta_1 = 8/3\pi$.

$$\therefore \quad \bar{H}_c = H_c/\sin\theta_1 = 3\pi H_c/8 = 1.18H_c \qquad 26)$$

Although this estimate of $\bar{H}_c$ is an upper limit the error is clearly not large as we expect $\bar{H}_c > H_c$.

From 3), 24) and 26)

$$\bar{J}_{rs} = 2\bar{H}_c/3(N + 1/S) \qquad 27)$$

We now consider the coercivity of remanence $\bar{H}_{cr}$ of the assemblage. Following saturation, let $J(\theta_2) = 0$ when $H = \bar{H}_{cr}$. Then $\bar{H}_{cr}\sin\theta_2 = H_c$, or $\sin\theta_2 = H_c/\bar{H}_c/\bar{H}_{cr}$.

For $H = -\bar{H}_{cr}$: $J(\theta) = S\bar{H}_{cr}\left[\sin\theta_2 - \sin\theta\right]/(1/ + NS)$

The remanence is given by

$$J_r(\theta) = J(\theta) - J_{ind}(\theta)$$

$$\therefore \quad J_r(\theta) = S\bar{H}_{cr}\left[\sin\theta_2 - \sin\theta\right]/(1 + NS) + \chi_i\,\bar{H}_{cr}\sin\theta/(1 + N\chi_i)$$

$$\bar{J}_r = \int_0^{\pi/2} J_r(\theta)\sin\theta \cdot \sin\theta d\theta = S\bar{H}_{cr}\left[\pi\sin\theta_2/4 - 2/3\right]/(1 + NS) + 2\chi_i\bar{H}_{cr}/3(1 + N\chi_i) \qquad 28)$$

Substituting $\sin\theta_2 = H_c/\bar{H}_{cr}$ into 28)

$$\bar{J}_r = 2\bar{H}_{cr}\left[\chi_i/(1 + N\chi_i) - S/(1 + NS)\right]/3 + \pi SH_c/4(1 + NS)$$

The condition $\bar{J}_r = 0$ gives, taking into account 13)

$$\bar{H}_{cr} = (1 + N\chi_i)\ (3\pi H_c/8)/(1 - \chi_i/S) = 1.18H_{cr} \qquad 29)$$

$$\therefore\ \bar{H}_{cr} = (1 + N\chi_i)\ \bar{H}_c/(1 - \chi_i/S) \qquad 30)$$

which is identical in form to 13).

Substituting 23) into 30) gives

$$\bar{H}_{cr} = 2\bar{H}_c/\ [2 - 3\bar{\chi}_o\ (N + 1/S)] \qquad 31)$$

In order to obtain an expression for the coercivity of remanence acquisition $\bar{H}'_{cr}$ of the assemblage we assume the initial magnetisation curve obeys Rayleigh's relations up to $J_r = J_{rs}/2$. Therefore $H_e = \bar{H}'_{cr}$

$$J_r(\theta) = (1/2)\eta\ [\bar{H}(\theta)]^2 = (1/2)\eta\ (\bar{H}'_{cr}\sin\theta)^2 \qquad 32)$$

Where η is the Rayleigh coefficient, which is obtainable from the relationships pertaining to the basal plane

$J_r = J_{rs}/2 = (1/2)\eta\ (H'_{cr})^2$

$$\therefore\ \eta = J_{rs}/(H'_{cr})^2 \qquad 33)$$

From 32) and 33): $J_r(\theta) = (1/2)J_{rs}\ (\bar{H}'_{cr}/H'_{cr})^2\ \sin^2\theta$

$$\therefore\ \bar{J}_r = (1/2)J_{rs}\ (\bar{H}'_{cr}/H'_{cr})^2\ \overline{\sin^3\theta} = (3\pi J_{rs}/32)(\bar{H}'_{cr}/H'_{cr})^2$$

From the definition of $\bar{H}'_{cr}$, $\bar{J}_r = \bar{J}_{rs}/2 = \pi J_{rs}/8$ when $H_e = \bar{H}'_{cr}$

$$\therefore \quad (\bar{H}'_{cr}/H'_{cr}) = 4/3$$

$$\bar{H}'_{cr} = 1.15\ H'_{cr} \qquad 34)$$

Substituting 19) into 34)

$$\bar{H}'_{cr} = 1.15\ (H_{cr} + NJ_{rs}/2(1 - N\chi_o)) \qquad 35)$$

Using 3) $$\bar{H}'_{cr} = 1.15\ \left[\bar{H}_{cr} + NH_c/(2(N+1/S)(1-N\chi_o))\right] \qquad 36)$$

Substituting 26) and 29) into 36)

$$\bar{H}'_{cr} = (1.15/1.18)\ \left[\bar{H}_{cr} + N\bar{H}_c/(2(N+1/S)(1-N\chi_o))\right] \qquad 37)$$

Also, from 23), 24), 26) and 35)

$$\bar{H}'_{cr} = 0.98\ \left[\bar{H}_{cr} + 3N\bar{J}_{rs}/(4-6N\bar{\chi}_o)\right] \qquad 38)$$

$$\therefore \quad \bar{H}'_{cr} - \bar{H}_{cr} \approx 3N\bar{J}_{rs}/(4-6N\bar{\chi}_o) \qquad 39)$$

Solving for N: $$N = 4(\bar{H}'_{cr} - \bar{H}_{cr})/\left[3\bar{J}_{rs} + 6\bar{\chi}_o(\bar{H}'_{cr} - \bar{H}_{cr})\right] \qquad 40)$$

Thus the within-basal plane self-demagnetising factor N is in principle determinable from the observed hysteresis

parameters $\bar{H}'_{cr}$, $\bar{H}_{cr}$, $\bar{J}_{rs}$ and $\bar{\chi}_o$.

The parameter S may then be calculated from 27) as

$$S = [2\bar{H}_c/3\bar{J}_{rs} - N]^{-1}$$

However S is difficult to determine accurately as it depends on the difference of two similar quantities. Measurements of $\bar{H}_c$ are biased towards the softer grains and the consequent underestimation can lead to large errors in S.

For the randomly oriented assemblage the relationship corresponding to 15) is identical in form, viz:

$$\bar{H}_{cr} = \bar{J}_{rs}\bar{H}_c/(\bar{J}_{rs}-\bar{\chi}_o\bar{H}_c) \qquad 42)$$

For a randomly oriented assemblage the median destructive field of SIRM depends on the mode of AF demagnetisation. For a fixed peak field, tumbling demagnetisation is more effective than 3-axis demagnetisation, which in turn is more effective than single-axis demagnetisation (McFadden, 1981). In the case of tumbling demagnetisation all grains are exposed to the peak field. Therefore in this case $\bar{H}_{\frac{1}{2}} = H_{\frac{1}{2}}$.

From 17): $\bar{H}_{\frac{1}{2}} = H_{cr} - NJ_{rs}/2(1-N\chi_o)$

Using 22), 24) and 29):

$$\bar{H}_{\frac{1}{2}} = (8/3)[\bar{H}_{cr} - 3N\bar{J}_{rs}/(4-6N\bar{\chi}_o)] \quad \text{(tumbling)} \qquad 43)$$

Substituting 39) into 43)

$$\bar{H}_{\frac{1}{2}} \simeq 0.85\ (2\bar{H}_{cr} - \bar{H}'_{cr}) \quad \text{(tumbling)} \qquad 44$$

We now consider single-axis demagnetisation of SIRM, where the demagnetisation is along the SIRM direction. Only the field component in the basal plane of a grain is effective in demagnetising the grain. Calculation of the effective mdf of the assemblage in this case requires a model for the coercivity spectrum of the grains or, equivalently, knowledge

of the average slope (the incremental susceptibility) of the minor hysteresis loops around which the grains are taken during AF demagnetisation.

Fig. 2b illustrates this point. Initially as the effective external field $H_e \rightarrow -\bar{H}_{\frac{1}{2}}\sin\theta$, the grain descends the side of the saturation loop and the magnetisation decreases from J_{rs} to $J_1(\theta)$. The grain then travels around the minor loop with average slope χ, the magnetisation varying between $J_1(\theta)$, and $J_2(\theta)$ as the effective applied field varies between the limits $\pm\bar{H}_{\frac{1}{2}}\sin\theta$. In general we expect χ to depend on the initial magnetisation $J_1(\theta)$ of the minor loop, and hence on θ. If χ is constant and equal to χ_i, consideration of similar triangles in Fig. 2b gives for the field component $H_{1/n}$ required to reduce the SIRM to 1/n of its initial value: $H_{1/n} = H_{cr}(1-1/n)$. This corresponds to a linear demagnetisation curve and a uniform AF coercivity spectrum. In particular for this case $H_{\frac{1}{2}} = H_{cr}/2$ and $\bar{H}_{\frac{1}{2}} = \bar{H}_{cr}/2$. Real demagnetisation curves are generally concave upwards and approximately exponential in form, implying χ is not constant.

However, since we have established that the ratios $\bar{H}_c/H_c$, $\bar{H}_{cr}/H_{cr}$ and $\bar{H}'_{cr}/H'_{cr}$ are almost equal, averaging 1.17, it is reasonable to expect that $\bar{H}_{\frac{1}{2}}$ is slightly more than $H_{\frac{1}{2}}$ by about the same factor. Therefore the relationships 20) and 21) should hold approximately for randomly oriented assemblages.

$$\therefore \quad \bar{H}'_{cr} + \bar{H}_{\frac{1}{2}} \simeq 2\bar{H}_{cr} \quad \text{(single-axis)} \qquad 45)$$

From 44) and 45) we have

$$\bar{H}_{\frac{1}{2}}(\text{tumbling})/\bar{H}_{\frac{1}{2}}(\text{single-axis}) \simeq 0.85 \qquad 46)$$

We now consider the approach to saturation of a randomly oriented assemblage. Within the basal plane the approach of the magnetisation to technical saturation goes approximately as $J_s\left[1-b/H^2\right]$ (Chikazumi and Charap, 1978, p.275), where b is related to magnetocrystalline anisotropy constants. Assuming all grains are in the range of rotation magnetisation where this relationship is obeyed, the magnetisation of a grain at angle θ to H is $J_s\left[1-b/(H\sin\theta)^2\right]$.

Integrating over all orientations gives

$$\bar{J} = J_s\int_0^{\pi/2}\left[1 - b/H^2\sin^2\theta\right]\sin^2\theta\,d\theta = J_s\left[\pi/4 - \pi b/2H^2\right]$$

The saturation magnetisation of the assemblage is $J_s\overline{\sin\theta} = \pi J_s/4$

$$\therefore\quad \bar{J} = \bar{J}_s\left[1 - 2b/H^2\right] \qquad 47)$$

It follows immediately from 47) that $\bar{b} = 2b$ 48)

2 Magnetic hysteresis parameters of SD grains

The hysteresis properties of SD grains which have an easy plane of magnetisation have been discussed by Dunlop (1971) with regard to fine-grained haematite. He considers the cases of uniaxial, trigonal and triaxial (hexagonal) anisotropy within the basal plane. The results for uniaxial anisotropy pertain to SD pyrrhotite, the orthorhombic a-axis defining the easy direction of magnetisation.

Magnetocrystalline anisotropy dominates the basal plane

anisotropy of SD pyrrhotite, shape and strain anisotropies being relegated to a secondary role. The maximum shape anisotropy $K_s = \pi J_s^2 \simeq 3 \times 10^4$ erg/cm^3 for needle-like grains, whereas for a stress σ of 10^9 dyne/cm^2 the strain anisotropy $K_\sigma = \lambda\sigma \sim 10^4$ erg/cm^3. These values compare with $K_1 \sim 3 \times 10^5$ erg/cm^3 for magnetocrystalline anisotropy.

In section .1 we considered the case where the applied field is insufficient to pull the grain moments out of the basal plane and this assumption will also apply to the discussion of SD grains. For pyrrhotite the anisotropy field along $[\bar{0}0\bar{1}]$ is given by $H_A \simeq 2K_3/J_s \sim 60$kG, so the assumption is justified for hysteresis properties measured in fields up to ~10kG. Dunlop (1971) also treats the alternative extreme where the grain moments are pulled out of the basal plane into perfect alignment with the field.

SD pyrrhotite grains have zero low field susceptibility along the a-axis and negligible susceptibility along the c-axis. The susceptibility along the b-axis is found by minimising the total energy (magnetostatic + magnetocrystalline) for a field H along the b-axis. Denote the azimuthal angle of the grain magnetic moment within the basal plane, measured from the a-axis, by ϕ. The stable position of the moment is then obtained by differentiating $E = K_1 \sin^2\phi - HJ_s \sin\phi$, and equating to zero.

This gives $\sin\phi = HJ_s/2K_1$

The induced magnetisation component parallel to H is $J_s \sin\phi$.

$$\therefore \quad \chi_b = J_s \sin\phi / H = J_s^2/2K_1 \qquad 49)$$

In order to calculate the susceptibility of a randomly oriented assemblage, it is simpler to consider a fixed grain and a randomly oriented field direction. If $\tilde{H}$ makes an angle θ with the c-axis the component of $\tilde{H}$ along the b-axis is $H\sin\theta\sin\phi$, where ϕ is the angle from the a-axis to the basal plane projection of $\tilde{H}$, as above. The induced magnetisation along the b-axis is then $\chi_b H\sin\theta\sin\phi$ and the component of induced magnetisation along $\tilde{H}$ is then $\chi_b H\sin\theta\sin\phi \cdot \sin\theta\sin\phi$. Therefore the effective susceptibility along the direction (θ,ϕ) is $\chi_b \sin^2\theta\sin^2\phi$.

By symmetry it is only necessary to integrate over a hemisphere, giving

$$\bar{\chi} = (1/2\pi)\int_0^{2\pi}\int_0^{\pi/2} \chi_b \sin^2\theta\sin^2\phi\, d\theta\, d\phi$$

$$\therefore \quad \bar{\chi} = \chi_b/3 = J_s^2/6K_1 \qquad 50)$$

When $\tilde{H}$ is along the b- or c-axis the grain exhibits no hysteresis. The total energy of a grain magnetised initially along $[\bar{1}00]$ with a back field $\tilde{H}$ along $[\bar{1}\bar{0}0]$ is $E=K_1\sin^2\phi + HJ_s\cos\phi$. Consideration of conditions for stable equilibrium gives for the critical field required to reverse the magnetisation, $H_c = 2K_1/J_s$. The coercive force $\bar{H}_c$ of the randomly oriented assemblage is approximately $H_c/2$.

$$\therefore \quad \bar{H}_c \simeq K_1/J_s \qquad 51)$$

Substituting numerical values (J_s = 93G, $K_1 = 3 \times 10^5 erg/cm^3$) into 50) and 51) gives $\bar{\chi} = 4.8 \times 10^{-3}$ and $\bar{H}_c$ = 3,200 Oe.

Dunlop (1971) gives the following expression for $\bar{H}_{cr}$

$$\bar{H}_{cr} = 1.29K_1/J_s \qquad 52)$$

3 Self-demagnetisation of MD Grains

Theories of hysteresis and thermoremanence of MD grains have hitherto relied on certain assumptions concerning the effects of self-demagnetisation (e.g. Néel, 1955; Stacey and Banerjee, 1974). Although the self-demagnetising field of inhomogenously magnetised grains is non-uniform, an averaged back-field has been implicitly considered to control the properties of the grains, and self-demagnetising factors derived for uniformly magnetised ellipsoids which approximate the (generally irregular) shapes of the grains have been used for quantitative analysis. The ellipsoidal approximation is justified for SD grains, as an equivalent ellipsoid can be found with axial ratios such that the total magnetostatic energy (self-energy plus potential energy in the applied field) is always equal to that of a uniformly magnetised irregular grain of the same volume (Brown and Morrish, 1957). However this result does not hold for inhomogeneous magnetisation.

Merrill (1977, 1981) has criticised conventional MD theories and has shown that, far from being constant and uniquely determined by grain shape, the effective self-demagnetising factor must vary with the magnetisation and be highly sensitive to domain structure. For example, the magnetostatic energy density for a platy two domain grain magnetised along the short axis decreases as the oblateness of the grain increases - behaviour which is precisely opposite to that for a uniformly magnetised grain. The effective self-demagnetising factor is a minimum when the grain is in the demagnetised state, approaching the value applicable to

SD grains as the applied field increases and the domain wall moves towards the edge of the grain.

However, as the number of domains in a grain becomes large the self-demagnetising factor approaches that for a uniformly magnetised grain of the same shape. It is intuitively reasonable that, as free magnetic poles of opposite sign at the grain surface become more intimately intermixed, the averaged self-demagnetising field becomes essentially determined by the nett surface pole density or, which comes to the same thing, by the bulk magnetisation. It is for this reason that shape anisotropy of SD grains is a meaningful concept, in spite of the gross inhomogeneity of magnetisation on an atomic scale, and magnetometric measurements on macroscopic ellipsoidal specimens of permeable materials conform closely to theory, although the magnetisation is non-uniform on a microscopic scale.

It follows that conventional shape-dependent demagnetising factors may be a reasonable approximation for sufficiently large MD grains, but will fall down for grains containing only a few domain walls. Particularly for small MD grains, additional complications concern possible inadequacy of averaged values of N if magnetisation processes are controlled by local fields acting on domain walls and interdependence of domain wall displacements involving co-operative behaviour.

Support for these arguments can be found both in experimental measurements on MD grains and in some rigorous theoretical results. Besnus (1962) determined the magnetisation curve for a large pyrrhotite crystal in the form of a sphere

3.9 mm in diameter. For the initial magnetisation curve the results imply an empirical value of $4\pi/3$ for N, in agreement with the value for uniform magnetisation. Because the self-demagnetising factor is also $4\pi/3$ when the grain is saturated, N must have a minimum value at some intermediate field strength, when there are only a few domain walls remaining.

Kooy and Enz (1960) derived the surface density of magnetostatic energy for an infinite plate containing lamellar domains of alternating polarity, magnetised normal to the plate. The theory was substantiated by measurements on a thin platelet of barium hexaferrite. From the theoretical expression for magnetostatic energy it is easily shown that N approaches 4π as the width of the domains becomes small compared to the plate thickness. This theory has been generalised by Craik and McIntyre (1969).

We now turn to the problem of empirical estimation of self-demagnetising factors for dispersions of MD grains. Smith and Merrill (1982) have shown that attempts (e.g. Parry, 1980) to estimate N from the relationships $J_{rs} = H_c/N$ and $H_{cr} = H_c/(1-N\chi_0)$ are, firstly, not independent and, secondly, are inaccurate if the sides of the saturation intrinsic hysteresis loop depart significantly from the vertical.

The theory developed in Section 1 offers a method for estimation of an average value of N for an assemblage of MD grains. It must be stressed that a number of assumptions are involved in the derivation of eq. 40 which may lead to inaccuracies in values of N deduced from experimental

data. We have assumed that a single value of N is applicable to a grain in the initially demagnetised state, along the critical magnetisation curve up to $J = J_{rs}/2$ and in the vicinity of the coercive force point. Although this is not strictly true the variations should be small for grains containing many domains. For small MD grains the empirical value of N will represent some sort of average around the hysteresis loop. We have also assumed linearity of reversible magnetisation in applied field and we have neglected curvature of the sides of the hysteresis loop.

The experimental data offer support for approximate validity of these assumptions. Values of $\bar{\eta}$ estimated from IRMs acquired in 50 - 100 oe using eq. 2* are only slightly lower than those determined in the range 0 - 10 oe, even though Rayleigh's relations are only strictly satisfied in fields which are small compared to H_c. This is consistent with linearity of reversible magnetisation from 0 to ~100 oe, and possibly beyond. The close agreement between measured and calculated values of H_{cr} (Table 6*) confirms eq. 42 and demonstrates self-consistency of the theory. The agreement between eq. 45 and the experimental results (Table 6*) also gives general support to the assumptions of the theory, but in particular lends credence to the argument relating H_{iD} and H'_{cr}. It should be noted that the ratio $(H'_{cr} - H_{cr})/(H_{cr} - H_{½})$ is a more sensitive indicator of discrepancies between theory and experiment and for some specimens (notably R12, R14 and R16) this ratio departs significantly from the predicted value of unity.

An experimental result which is not in very good accord with the theory involves the relationship between median destructive fields for tumbling and single-axis demagnetisation. The empirical values of $H'_{\frac{1}{2}}/H_{\frac{1}{2}}$ are about 0.6, significantly less than the value of 0.85 predicted by eq. 46.

The theory of Section .1 should therefore be regarded as semi-quantitative. It offers an explanation of the empirical relationship $H_{\frac{1}{2}} < H_{cr} < H'_{cr}$ for MD grains, and allows at least an order-of-magnitude empirical estimate of N. This is particularly important because rigorous alternatives appear to be lacking (Smith and Merrill, 1982).

Dankers (1981) did not consider self-demagnetisation in analysing his experimental results. Instead he invoked magnetostatic interactions between grains to explain the relationship 45) which he found to apply to MD magnetite and titanomagnetite. This was by analogy with the case of interacting SD particles (for which $H_{\frac{1}{2}} < H_{cr}$). However Dankers' explanation is based on an erroneous interpretation of the local field acting on a grain (see Brown (1962, pp. 38-42) for discussion of local fields). Furthermore for particular magnetite grain size fractions H'_{cr} tends to decrease and $H_{\frac{1}{2}}$ tends to increase with packing density, whereas increasing the magnetite content should increase $H'_{cr}/H_{\frac{1}{2}}$ if grain interactions are responsible for the behaviour described by 45). The work of Luce (1980) also suggests that the role of interactions in rock magnetism may have been commonly exaggerated. On the other hand, the experimental results are readily

explained on the basis of self-demagnetisation because higher packing densities lower the effective self-demagnetising factor (Morrish and Watt, 1957). From 20) and 10) $H'_{cr} - H_{cr} = NJ_{rs}(1 + N\chi_i)/2$ which clearly decreases monotonically as N decreases with higher packing density.

Applying eq. 18 to the data of Parry (1980) we deduce $N \simeq 3$ for magnetite grains ranging from 220μm to 1.5μm. This is in good agreement with the values calculated by that author on the basis of theoretical relationships given by Stacey and Banerjee (1974), which explicitly assume $S = \infty$. The reason for this agreement is that $\chi_i \sim 1$ for MD magnetite, $S >> \chi_i$ and therefore $N + 1/S \simeq N$. For the case of pyrrhotite, however, neglect of the finite slope of the intrinsic hysteresis loop around the coercive force point leads to large errors in estimation of N.

Estimates of N, S and S/χ_i for each of the sized pyrrhotite specimens are given in Table 1. Except for the coarsest grains 1/S is comparable to, or exceeds, N and the simplified theory of Stacey and Banerjee (1974) clearly breaks down. Errors in the cited values are difficult to estimate. Values of N greater than ~4 for the coarser grain sizes seem rather high, although they do not exceed conceivable bounds. If the assumptions of Section 1 were totally unrealistic there would be no reason for eq. 40 to yield sensible values for N. This in itself gives some confidence in the reasoning of Section 1. For the cases where N is ill-defined due to departures from ideal behaviour (specimens R12 - R16) the upper values are preferred as they are more consistent with values for the other specimens.

S is almost certainly overestimated because of the tendency for H_c to be biased towards the softer grains in an assemblage. This effect is most severe for the coarser grain sizes, and becomes much less significant for $S<<1$ (e.g. for specimens R12 - R17).

4 Domain Structure in monoclinic pyrrhotite

Besnus (1959, 1966) has described the domain structure of large crystals of monoclinic pyrrhotite as revealed by the Bitter pattern technique. Natural crystals are almost invariably twinned - consisting of approximately equal proportions of lamellar twins (~3μm thick) with orthorhombic symmetry parallel to the basal plane of the pyrrhotite structure. The twins are stacked along the c-axis with an angle of 120° between the a-axes of successive members, producing an overall hexagonal symmetry for the crystal. Each twin is subdivided into rod-like magnetic domains parallel to the easy direction, separated by 180° walls which contain the a- and c- axes. Closure domains are rare. This simple domain structure is readily understood on the basis of the strong uniaxial basal plane anistropy and the relatively low spontaneous magnetisation of pyrrhotite.

Soffel (1977, 1981) has described domain structures in small pyrrhotite grains (<2μm - 200μm). Because of the low magnetostriction of pyrrhotite, domain structure was clearly revealed by magnetic colloid distribution (Bitter patterns) on mechanically polished surfaces. Special techniques such as ionic polishing to obtain strain-free surfaces were unnecessary. A simple domain structure consisting essentially of parallel rod-like or sheet-like domains was observed down to the critical SD size of ~1.6μm. Observation of wall movement in applied fields revealed a wide range of critical fields for different domain walls within grains. Higher coercivities, corresponding to pseudo single domain (PSD) effects, were associated with walls whose motion is impeded

by non-magnetic inclusions or surface irregularities.

Halgedahl and Fuller (1981) studied domain structure in polycrystalline pyrrhotite. The domain pattern was found to depend on the method employed to demagnetise the specimen. Following AF demagnetisation a simple structure was observed with rod-like or sheet-like domains separated by straight parallel 180° walls. However, after thermal demagnetisation the pattern was less regular, the 180° walls were somewhat undulatory and individual domains were truncated by irregular, extremely mobile walls which could be displaced in a few oersteds. The 180° walls, on the other hand, require fields of several tens of oersteds to be visibly displaced. This work provides an excellent illustration of the long recognised fact that magnetic properties of materials depend on the path by which the initially demagnetised state is attained.

We now proceed to calculate domain wall width and energy in pyrrhotite. A 180° wall in pyrrhotite consists of parallel planes, normal to the orthorhombic b-axis, separated by $b/4 = A/2$.

In successive planes the spins rotate progressively out of the basal plane, maintaining antiparallelism in alternate layers along the c-axis. This gradual rotation of spins out of the easy plane incurs a considerable increase of magnetocrystalline anistropy energy but avoids production of free poles within the wall, and is therefore favoured over rotation of spins within the basal plane (which would have magnetisation with non-zero divergence, thereby increasing the magnetostatic energy).

Adopting the approximation of constant small increments ε in angle from the basal plane in successive planes of spins (cf. Stacey and Banerjee, 1974, pp. 53-55), the excess exchange energy of a line of n spins of magnitude S is $J_e S^2 \varepsilon^2 n = J_e S^2 \pi^2 / n$ where J_e is the exchange integral.

Each layer of the wall consists of a rectangular array of spins with lattice constants $\sqrt{3}A$ and $C/2$, so unit area of the wall contains $1/(\sqrt{3}A.C/2) = 2/\sqrt{3}AC$ spins.

The exchange energy per unit area of wall is therefore

$$E_{ex} = 2J_e S^2 \pi^2 / \sqrt{3} \quad nAC \qquad (53)$$

The anisotropy energy density at any point within the wall is $K_3 \sin^2\psi + K_4 \sin^4\psi$, where ψ is the angle between the spins and the easy direction. Averaging throughout the wall the anisotropy energy per unit volume of the wall is therefore

$$\overline{K} = (1/\pi) \int_0^{\pi} (K_3 \sin^2\psi + K_4 \sin^4\psi)\, d\psi = (4K_3 + 3K_4)/8$$

The anisotropy energy per unit area is then

$$E_{aniso} = (4K_3 + 3K_4)/8 \cdot (nA/2) = nA(4K_3 + 3K_4)/16 \qquad (54)$$

Differentiating the total energy with respect to n and equating to zero gives

$$n = (4\pi/A)\, [2J_e S^2/C\sqrt{3}\, (4K_3 + 3K_4)]^{\frac{1}{2}} \qquad (55)$$

The domain wall thickness $\delta = nA/2$

$$\therefore \delta = 6.8 \left[J_e S^2/C \ (4K_3 + 3K_4)\right]^{\frac{1}{2}} \qquad 56)$$

The wall energy per unit area is

$$\gamma = E_{ex} + E_{aniso} = (\pi/2) \left[2J_e S^2 (4K_3 + 3K_4)/C\sqrt{3}\right]^{\frac{1}{2}}$$

$$\therefore \quad \gamma = 1.7 \left[J_e S^2 (4K_3 + 3K_4)/C\right]^{\frac{1}{2}} \qquad 57)$$

Taking $J_e/k = 20K$, $k = 1.38 \times 10^{-16}$ erg/K, $S = 1.2$, $C = 6 \times 10^{-8}$ cm and $4K_3 + 3K_4 = 2 \times 10^7$ erg/cm^3 gives $\delta \simeq 4 \times 10^{-7}$cm = 40AU and $\gamma \simeq 1.9$ erg/cm^2. The wall is therefore quite thin ($n \simeq 24$, $\delta \simeq 12$A) due to the large magnetocrystalline anisotropy. The wall energy is typical of ferro- and ferrimagnetic substances.

The critical SD size d_c is given by (Stacey and Banerjee, 1974, p.59)

$$d_c \simeq 1.3\gamma/J_s^2 \qquad 58$$

Substitution of numerical values gives $d_c = 2.9\mu$m for pyrrhotite. Soffel (1977) found empirically $d_c \simeq 1.6\mu$m, which corresponds to $\gamma = 1$ erg/cm^2. In view of all the uncertainties surrounding theoretical estimation of d_c the agreement between theory and experiment is satisfactory.

Now let us consider a cubic grain of side d containing n′ lamellar or rod-like domains. The magnetostatic energy per unit cross-section area E_m of a large grain with lamellar or checkerboard domain structure is proportional to the domain width $d_o = d/n'$ (Chikazumi and Charap, 1978, p.211).

$$\therefore E_m = \alpha d/n' \qquad 59)$$

where α is a constant dependent on the domain geometry. There are $n'-1$ domain walls each with wall energy γd^2. Therefore the domain wall energy per unit cross-section area is given by

$$E_\omega = (n'-1)\gamma d^2/d^2 \simeq n'\gamma \qquad 60)$$

The total surface density of energy E is

$$E = E_m + E_\omega = (\alpha d/n') + n'\gamma \qquad 61)$$

The value of n' which minimises the total energy for given grain size is found by differentiating E with respect to n' and equating to zero, giving

$$n' = (\alpha d/\gamma)^{\frac{1}{2}} \qquad 62)$$

$$\therefore d_o = d(\gamma/\alpha d)^{\frac{1}{2}} = (\gamma d/\alpha)^{\frac{1}{2}} \qquad 63)$$

From 63) we expect the domain width in MD grains to vary approximately as the square root of the grain size. The empirical relationship between n' and d found by Soffel (1977) is in reasonable agreement with 62). Taking the mean size of grains containing 10 domains as 50μm gives

$$n' \simeq 1.4d^{\frac{1}{2}}$$

(dimensions in μm) 64)

$$d_o \simeq 0.7d^{\frac{1}{2}}$$

5 Coercive force and intrinsic susceptibility

The susceptibility and coercive force of a randomly oriented assemblage of stable SD grains are given by 50)

and 51) respectively. In MD grains domain wall displacement contributes to the intrinsic susceptibility along with domain rotation and the observed susceptibility is controlled by self-demagnetisation of the grains.

Coercive force in MD grains is due to energy barriers which impede domain wall movement and is therefore inversely correlated with susceptibility.

Theories of coercive force in MD materials fall into two categories: strain models and inclusion models. In strain models H_c is correlated with magnetostriction λ, whereas in inclusion models H_c is dominantly controlled by magnetocrystalline anistropy.

Although there are many variants of these basic types of model the general features of MD theories of coercive force are well illustrated by the dispersed field models of Néel (1946, 1949). The energy of a domain wall is envisaged to vary with position due to fluctuations in direction and magnitude of J_s associated with inhomogeneously distributed stresses and non-magnetic inclusions. The expressions given are

$$\text{Strain:}\quad H_c \simeq 0.19\lambda^2 s^2 f' [1.39 + \ln(1+2\pi J_s^2/|K|)^{\frac{1}{2}}] / |K| J_s \qquad 65)$$

$$\text{Inclusions:}\quad H_c \simeq 2|K| f [0.39 + \ln(1+2\pi J_s^2/|K|)^{\frac{1}{2}}] / \pi J_s \qquad 66)$$

where f' is the volume fraction affected by stress variations of magnitude S, and f is the volume fraction of inclusions.

The logarithmic terms in 65) and 66) differ from the final equations derived by Néel (1946) in that, for the cases considered by him, the arguments of the logarithms are much greater than one and the additive term of unity could be neglected, whereas we require the more general form. The order of magnitude of the numerical constants in these equations is not significantly affected by the different approximations applicable to iron and nickel, on the one hand, and pyrrhotite on the other.

Substitution of numerical values ($\lambda=10^{-5}$, $s=10^9$ dyne/cm^2, $K=K_3=3\times10^6$ erg/cm^3, $J_s=93$G) into 65) and 66) gives $H_c \simeq 0.1f'$ and $H_c \simeq 8200\,f$ respectively. Clearly strain models cannot account for the coercive force of MD pyrrhotite, even when rather high internal stresses are assumed. On the other hand relatively small volume fractions of inclusions can explain the observed coercive force of MD pyrrhotite. The pinning of domain walls by non-magnetic inclusions in pyrrhotite has been directly demonstrated by Soffel (1977).

Although the calculations above can give the correct order of magnitude for the coercive force of bulk materials they do not take into account the dependence of fluctuations of wall energy density with wall area, and hence with grain size. Experimentally it is found that $H_c \propto d^{-n}$, where $n \simeq 0.8$ for pyrrhotite grains smaller than about 100μm.

Stacey and Banerjee (1974, pp.66-69) show that $n = \ell(1-m)$, where ℓ is related to domain geometry and m depends on the distribution of the crystal defects which control the coercive force. The parameter ℓ varies from

zero if domain size is independent of grain size to a maximum of two if lamellar domains extend right across the grain, whereas m varies from 0.5 if the defects are randomly distributed to 1 for a perfectly ordered array of defects. If we assume lamellar domain structure, we have $m \simeq 0.6$ suggesting that the inclusions which are responsible for H_c are more or less disordered in pyrrhotite.

The intrinsic susceptibility χ_b parallel to the b-axis of an untwinned pyrrhotite grain is given by 49) as $93^2/6\times10^5 = 1.44\times10^{-2}$. Due to self-demagnetisation, in MD grains this is reduced to an effective value $\chi_b/(1+N\chi_b)$. The contribution of domain moment rotation to the observed susceptibility of a random assemblage is one third of this, or $\chi_b/3(1+N\chi_b)$. Similarly the contribution of domain wall displacement to the observed susceptibility is $\chi_a/3(1+N\chi_a)$. N is assumed to be isotropic within the basal plane. Since the susceptibility along the c-axis is negligible, we have

$$\bar{\chi}_o = [\chi_a/(1+N\chi_a) + \chi_b/(1+N\chi_b)]/3 \qquad 67)$$

from which we obtain

$$\text{(Untwinned) } \chi_a = [3\bar{\chi}_o - \chi_b/(1+N\chi_b)]/[1-N(3\bar{\chi}_o - \chi_b/(1+N\chi_b))] \qquad 68)$$

Thus we can determine χ_a from $\bar{\chi}_o$.

Large grains may possess a triad twin structure with equal proportions of 120° twins. In this case the intrinsic susceptibility due to wall displacement is isotropic within

the basal plane and is equal to $\chi'_a = (1/3)\ (\chi_a + 2\chi_a \cos^2 120^o) = \chi_a/2$. Similarly $\chi'_b = \chi_b/2$. The isotropic intrinsic susceptibility within the basal plane is therefore $\chi_i = (\chi_a+\chi_b)/2$. From 23) we have

$$3\bar{\chi}_o/2 = \chi_i/(1+N\chi_i) = (\chi_a+\chi_b)/(2+N(\chi_a+\chi_b)) \qquad 69)$$

which gives

$$\text{(Triad structure)}\ \chi_a = 6\bar{\chi}_o/(2-3N\bar{\chi}_o) - \chi_b \qquad 70)$$

Calculated values of χ_a for the specimens containing only MD grains, based on data in Tables 2* and 1, are given in Table 2. In all cases $\chi_a > \chi_b$, implying that magnetisation processes in low fields are dominated by domain wall displacement, particularly for the larger grains. The calculated values of χ_a are slightly lower if a triad twin structure is assumed than if the grains are assumed to be untwinned.

The quality $\chi_a H_c$ is practically independent of grain size from ~7μm to ~80μm. A simplified model of domain wall displacement (Stacey and Banerjee, 1974, pp.73-74) leads to the expression

$$\chi_a H_c = (n'/v)\ At J_s/\pi \qquad 71)$$

where n'/v is the number of favourably oriented domain walls of area A, and t is the average separation of the energy minima.

From Table 2, $\chi_a H_c \sim 12$. Substituting this into 71) with $n' = 10$ for a 50μm grain gives $t \sim 2\mu m$ and with $n' \simeq 1$ for a 2μm grain gives $t \sim 0.8\mu m$. These values for the typical

spacing of energy minima are an order of magnitude larger than for magnetite (~0.15μm). In magnetite energy barriers to wall motion appear to result from superposition of interactions between the wall and a partially ordered array of dislocations, each of which produces an energy well comparable in width to a domain wall (Stacey and Banerjee, 1974, pp.57-62). The difference in t for pyrrhotite and magnetite presumably reflects a difference in the mechanism controlling coercive force. It seems that the non-magnetic inclusions or zones of anomalous spontaneous magnetisation which pin domain walls in pyrrhotite may be quite large, up to several microns across.

The discreteness of stable domain wall positions gives rise to the Barkhausen effect (the manner by which initial magnetisation curves of ferromagnetics are not smooth, but consist instead of a number of small discontinuous jumps). Barkhausen discreteness is important in small pyrrhotite grains as it produces a strong PSD moment. The average displacement of the wall from the mid-point of a TD grain, which is the position corresponding to zero nett moment, is t/4 (Stacey and Banerjee, 1974, p.62). If we consider a cubic 2μm pyrrhotite grain with a single domain wall, the average PSD moment due to Barkhausen discreteness is $2J_sAt/4 \simeq 1.5\times10^{-10}$ emu, which is 20% of the moment the grain would have if it were uniformly magnetised and is comparable to the moment of a 1.2μm cubic SD grain.

By comparison the moment of the domain wall itself, which is directed along the c-axis perpendicular to the Barkhausen moment, is approximately $2J_sAS/\pi$ (Stacey and Banerjee, 1974,

pp.60-61). Numerical substitution gives 1.2×10^{-12} emu for the wall moment, which is therefore negligible compared to the Barkhausen moment along the a-axis.

6 Palaeomagnetic stability of pyrrhotite

Because of the relatively large coercive force of pyrrhotite grains smaller than 100μm we expect remanence carried by these grains to be very stable at ambient temperatures. In the absence of an applied field the remanence of an assemblage of identical grains approaches zero exponentially with time constant τ given by (e.g. Dunlop, 1976)

$$\tau = (1/2f_o) \exp (E/kT) \qquad 72)$$

where f_o is a frequency factor of the order of 10^{10} Hz and E is the energy barrier between stable states. Eq. 72) is cominated by the exponential factor and f_o, which is a weakly varying function of volume, temperature and coercive force, can be regarded as effectively constant.

For SD grains E is the energy barrier between easy directions of magnetisation. For SD pyrrhotite grains of volume v, $E = (K_1+K_2)v \approx 3.8 \times 10^5 v$. The SPM threshold size at 300K for spherical grains can be calculated by setting τ = 1s in 72). Solving for v gives 2.6×10^{-18} cm^3, corresponding to $d_{spm} = 1.7 \times 10^{-6}$cm (0.017μm). Precise knowledge of f_o is unnecessary as choosing $f_o = 10^{12}$Hz, for example, gives $d_{spm} = 1.8 \times 10^{-6}$cm, which is only slightly different from the value above. Similarly changing τ somewhat makes little difference to the calculated d_{spm}.

However grains only slightly larger than the SPM threshold size are very stable. For instance for 0.04μm grains $\tau \sim 10^{200}$s.

For the case of MD grains $E = v_{act} J_s H_c/2$, where v_{act} is the volume affected by a single thermal activation event (Dunlop, 1976). A TD grain 2μm across has $t \sim 0.8\mu m$, so $v_{act} \simeq 0.8 \times 10^{-4} \times 4 \times 10^{-8} \sim 3 \times 10^{-12}$ cm^3. Taking $J_s = 93G$, $H_c = 800$ oe and substituting into 72) gives a huge value for τ. Massive coarse grained pyrrhotite is much softer with, typically, $H_c \sim 10$ oe. However, even assuming v_{act} is no larger for this material than for small MD grains, 72) shows the remanence is unaffected by thermal agitation at ambient temperatures over geological time.

This conclusion must be drastically modified at higher temperatures. Because of the relatively low Curie temperature ($\sim 325^{\circ}C$) of pyrrhotite and the rapid decrease in J_s, K_1, K_2 and H_c as the Curie point is approached, pyrrhotite is easily reset by low grade thermal events. Considering again spherical 0.04μm grains which are very stable at 300K, $K_1 + K_2$ is $\sim 0.9 \times 10^5$ erg/cm^3 at T = 523K ($250^{\circ}C$) (Besnus, 1966), giving $\tau \sim 7 \times 10^7$s, or about 2 years. Clearly regional metamorphism attaining $\sim 250^{\circ}C$ would completely reset any palaeomagnetic signal carried by these grains.

The survival potential of primary NRM as a function of regional metamorphic grade is summarised in Table 3. The table shows, for example, that for a primary remanence to have survived prehnite facies metamorphism at 200°C for 10^6 years the laboratory unblocking temperature must be greater than 260°C.

Blocking contours for remanence carried by pyrrhotite are shown in the thermal activation nomogram (Fig. 3). This diagram is analogous to those of Dunlop and Buchan (1977) for magnetite and haematite. The contours are derived for SD grains by assuming a grain volume and calculating values of τ corresponding to chosen values of T, using eq. 72. Each contour corresponds to a different grain size. The temperature variation of J_s, K_1 and K_2 for monoclinic pyrrhotite are taken from Besnus (1966).

The left of the diagram where the contours have shallow slope (the B field) corresponds to grains which are easily reset at temperatures well below the original blocking temperature. Time is the dominant resetting factor in the B region, which is therefore characterised by viscous remanence.

By contrast, the A region (where the contours are steep) corresponds to thermally stable magnetisation. Temperature, not time, is most effective in resetting magnetisations in this region of the diagram. In the A region the laboratory unblocking temperature of magnetisation is a good indicator of the acquisition blocking temperature, whereas in the B region the laboratory unblocking temperature is much higher

than the temperature at which the magnetisation was acquired (assuming a prolonged acquisition period).

However monoclinic pyrrhotite is chemically unstable above ~250^{o} and natural remanence acquired on cooling will generally be thermochemical in nature. Thus the greater portion of the A region in Fig. 2 is not applicable to remanence carried by monoclinic pyrrhotite. Furthermore primary remanence cannot survive regional metamorphism above lower pumpellyite facies (T<250^{o}C).

7 Remanence intensity and Koenigsberger ratio

For an assemblage of randomly oriented identical uniaxial SD particles the thermoremanence acquired on cooling from above the blocking temperature T_B to room temperature in a low field H is given by (Stacey and Banerjee, 1974, p. 107)

(SD) $$J_{TRM} = v J_s J_s(T_B) H/3kT_B \quad (73)$$

Consider the case $v = 3 \times 10^{-16}$ cm^3 for which $T_B = 590$K and $J_s(T_B) = 6$G. Then $J_{TRM} = 3 \times 10^{-16} \times 93 \times 6H/(3 \times 1.38 \times 10^{-16} \times 590) = 0.7H$. Thus the intensity of TRM acquired in 0.5 oe is 0.35G.

Similarly for $v = 4.7 \times 10^{-18}$ cm , $T_B = 400$K and $J_{TRM} = 0.2H$. Therefore the TRM intensity of rocks containing only SD pyrrhotite grains should fall in the range 0.1f - 0.35f, where f is the volume fraction of pyrrhotite.

The corresponding Koenigsberger ratios are very high: $Q_{TRM} = J_{TRM}/kH = 40 - 150$ (using $k = 4.8 \times 10^{-3}$).

Chemical remanence, on the other hand, has intensity (Stacey and Banerjee, 1974, pp. 131-132)

$$\text{(SD)} \qquad J_{CRM} = J_s^2 \, H \ln (2f_o \tau)/3K_1 \simeq 0.2H \qquad 74)$$

with corresponding Koenigsberger ratio ~40.

Stacey and Banerjee (1974, pp. 107-106, 133) have also presented a simplified theory of TRM and CRM in large MD grains. Although the theory has flaws it is adequate for order of magnitude estimates of TRM and CRM intensities. Within the basal plane the magnetisation acquired is:

$$\text{(MD)} \qquad J_{TRM} = J_s H/NJ_s(T_B)(1+N\chi_{ab}) \qquad 75)$$

Where χ_{ab} is the intrinsic susceptibility within the basal plane. Hopkinson peaks on k-T curves and thermal demagnetisation data for coarse-grained pyrrhotite samples indicate that the blocking temperatures for MD grains lie mainly between 250°C and 300°C. This implies $J_s/J_s(T_B) \sim 3$. Taking N = 4 and $\chi_{ab} = 0.05$ gives $J_{TRM} \sim 0.6H$ or $J_{TRM} \sim 0.3G$ for H = 0.5 oe.

For a randomly oriented assemblage $\bar{J}_{TRM} \sim 0.4H$. The corresponding Koenigsberger ratio is $Q_{TRM} \simeq 0.4/(0.05 \times 2/3) = 12$. Observed susceptibilities of coarse-grained pyrrhotites range up to ~0.1, corresponding to $\chi_{ab} = 0.38$ (for N=4) Although this might seem to lower J_{TRM}, the blocking temperature, and therefore $J_s/J_s(T_B)$ may be higher. Syono et al. (1962) found for a large single crystal $\bar{J}_{TRM} \simeq 1.0H$.

CRM intensity is smaller than TRM intensity by the ratio $J_s(T_B)/J_s$. We have therefore $J_{CRM} \simeq 0.1G$ for H = 0.5 oe, and $Q_{CRM} \simeq 4$.

Smaller, and therefore harder, MD grains will have specific intensities and Koenigsberger ratios intermediate between those given here for large MD and SD grains.

It is apparent from the above discussion that theory can readily account for the intense remanence and high Koenigsberger ratios exhibited by many pyrrhotite-bearing rocks.

8. References

Besnus, M.J., 1959. Structure magnétique de la pyrrhotine. C.R. Acad. Sci., 248: 1634-1637.

Besnus, M.J., 1962. Lois d'aimantation de la pyrrhotine naturelle en fonction du champ. C.R. Acad. Sci., 254: 1587-1589.

Besnus, M.J., 1966. Propriétés magnétiques de la pyrrhotine naturelle. Thèse, Université de Strasbourg.

Brown, W.F., 1962. Magnetostatic Principles in Ferromagnetism. North-Holland, Amsterdam, 202pp.

Brown, W.F. and Morrish, A.H., 1957. Effect of a cavity on a single-domain magnetic particle. Phys. Rev., 105: 1198-1201.

Chikazumi, S. and Charap, S.H., 1978. Physics of Magnetism. Krieger, Huntington (N.Y.), 544pp.

Craik, D.J. and McIntyre, D.A., 1969. Anhysteretic magnetization processes in multidomain crystals and polycrystals. Proc. Roy. Soc. Lond. A., 313: 97-116.

Dankers, P., 1981. Relationship between median destructive field and remanent coercive forces for dispersed natural magnetite, titanomagnetite and hematite. Geophys. J. R. astron. Soc., 64: 447-461.

Dunlop, D.J., 1971. Magnetic properties of fine-particle hematite. Annales de Géophysique, 27: 269-293.

Dunlop, D.J., 1976. Thermal fluctuation analysis: a new technique in rock magnetism. J. Geophys. Res., 81: 3511-3517.

Dunlop, D.J. and Buchan, K.L., 1977. Thermal remagnetization and the paleointensity record of metamorphic rocks.. Phys. Earth Planet. Inter., 13: 325-331.

Halgedahl, S.L. and Fuller, M., 1981. The dependence of magnetic domain structure upon magnetization state in polycrystalline pyrrhotite. Phys. Earth Planet. Inter., 26: 93-97.

Kooy, C. and Enz, U., 1960. Experimental and theoretical study of the domain configuration in thin layers of $BaFe_{12}O_{19}$. Philips Res. Repts, 15: 7-29.

Luce, R.J., 1980. A theoretical study of fine-particle magnetization in rocks. Ph.D. thesis, University of Pittsburgh.

Merrill, R.T., 1977. The demagnetization field of multi-domain grains. J. Geomagn. Geoelectr., 29: 285-292.

Merrill, R.T., 1981. Toward a better theory of thermal remanent magnetization. J. Geophys. Res., 86: 937-949.

Morrish, A.H. and Watt, L.A.K., 1957. The effect of interaction between magnetic particles on the critical single-domain size. Phys. Rev., 105: 1476-1478.

Néel, L., 1946. Bases d'une nouvelle théorie générale du champ coercitif. Ann. Univ. Grenoble, 22: 299-343.

Néel, L., 1949. Nouvelle théorie du champ coercitif. Physica, 15: 225-234.

Néel, L., 1955. Some theoretical aspects of rock magnetism. Adv. Phys., 4: 191-243.

Parry, L.G., 1980. Shape related factors in the magnetization of immobilized magnetite particles. Phys. Earth Planet. Inter., 22: 144-154.

Smith, G. and Merrill, R.T., 1982. The determination of the internal magnetic field in magnetic grains. J. Geophys. Res., 87: 9419-9423.

Soffel, H., 1977. Pseudo-single-domain effects and single-domain multidomain transition in natural pyrrhotite deduced from domain structure observations. J. Geophys., 42: 351-359.

Soffel, H.C., 1981. Domain structure of natural fine-grained pyrrhotite in a rock matrix (diabase). Phys. Earth Planet. Inter., 26: 98-106.

Stacey, F.D. and Banerjee, S.K., 1974. The Physical Principles of Rock Magnetism. Elsevier, Amsterdam, 195pp.

TABLE 1 EMPIRICAL SELF-DEMAGNETISING FACTORS

Specimen	N (oe/G)	S (G/oe)	S/χ_i
NRC1	5.3	-	-
NRC2	5.5	6.8	150
NRC3	5.5	-	-
NRF	5.6	1.4	52
R4	4.7	0.75	25
R8	4.1	0.48	19
R12	2.7-3.7	0.23-0.29	11-14
R14	0.9-3.2	0.14-0.21	7.3-11
R16	0.5-2.5	0.09-0.11	5.5-6.5
R17	3.0	0.10	6.1
R18	3.9*	0.07*	3.7*

Notes:

(i) S is calculated from 41) and is undefined when $2\bar{H}_c/3\bar{J}_{rs} < N$ (NRC1 and NRC2)

(ii) When the data is in good agreement with eq. 20, N is calculated as $2(\bar{H}'_{cr} - \bar{H}_{\frac{1}{2}})/3[\bar{J}rs + \bar{\chi}_o(\bar{H}'_{cr} - \bar{H}_{\frac{1}{2}})]$

(iii) When 20) is not well satisfied by the data (for R12, R14, R16) two values of N are obtained by substituting $(\bar{H}'_{cr} - \bar{H}_{cr})$ and $(\bar{H}_{cr} - \bar{H}_{\frac{1}{2}})$ into 40). S and S/χ_i are then calculated for the corresponding values of N, using 41) and 23).

*R18 contains SD and SPM grains. Therefore the value of N calculated from MD theory will not represent a true self-demagnetising factor.

TABLE 2 INTRINSIC SUSCEPTIBILITY DUE TO WALL DISPLACEMENT

Specimen	$\chi_a \times 10^2$	$\chi_a' \times 10^2$	$\chi_a H_c$
NRC1 (83)	9.90	8.44	13.3
NRC2 (83)	8.72	7.58	12.2
NRC3 (83)	8.46	7.40	11.0
NRF (44)	4.17	3.99	8.8
R4 (42)	4.78	4.55	11.0
R8 (32)	3.60	3.52	10.1
R12 (20)	2.76	2.73	10.4
R14 (15.5)	2.60	2.58	13.3
R16 (11.1)	1.94	1.92	12.9
R17 (6.9)	1.84	1.83	15.1

Notes:

(i) χ_a is calculated from 68) and χ_a' from 70), in both cases taking the preferred value of N from Table 1.

(ii) Specimen R18 is omitted as domain wall displacement does not contribute to magnetisation processes in SD grains.

(iii) Mean grain sizes in microns are given in parentheses.

TABLE 3 SURVIVAL POTENTIAL OF PRIMARY NRM

Heating temperature* (°C)	Metamorphic grade	$(T_B)_{min}$ (°C)
100	Zeolite	195
150	Zeolite	225
200	Prehnite	260

*Temperature attained during metamorphic heating for 10^6 years.

$(T_B)_{min}$ = minimum laboratory unblocking temperature of primary NRM.

Fig. 1(a) Intrinsic hysteresis loop for a multi-domain pyrrhotite grain. The external and internal fields lie within the basal plane. Symbols are defined in the text.

1(b) Potential energy, E(x), of a domain wall of unit area in a multidomain grain. The energy arises from interaction of the wall with crystal defects and is a function of position. In the absence of an internal field the wall lies at an intrinsic energy minimum. When an internal field, H_i, acts on the wall it moves to an equilibrium position given by $2H_iJ = dE/dx$. If the field is then removed the wall drops back into the nearest intrinsic energy minimum, having undergone an irreversible displacement corresponding to change of magnetisation J_{irr}. The sense of the domain magnetisations and the field are indicated by arrows.

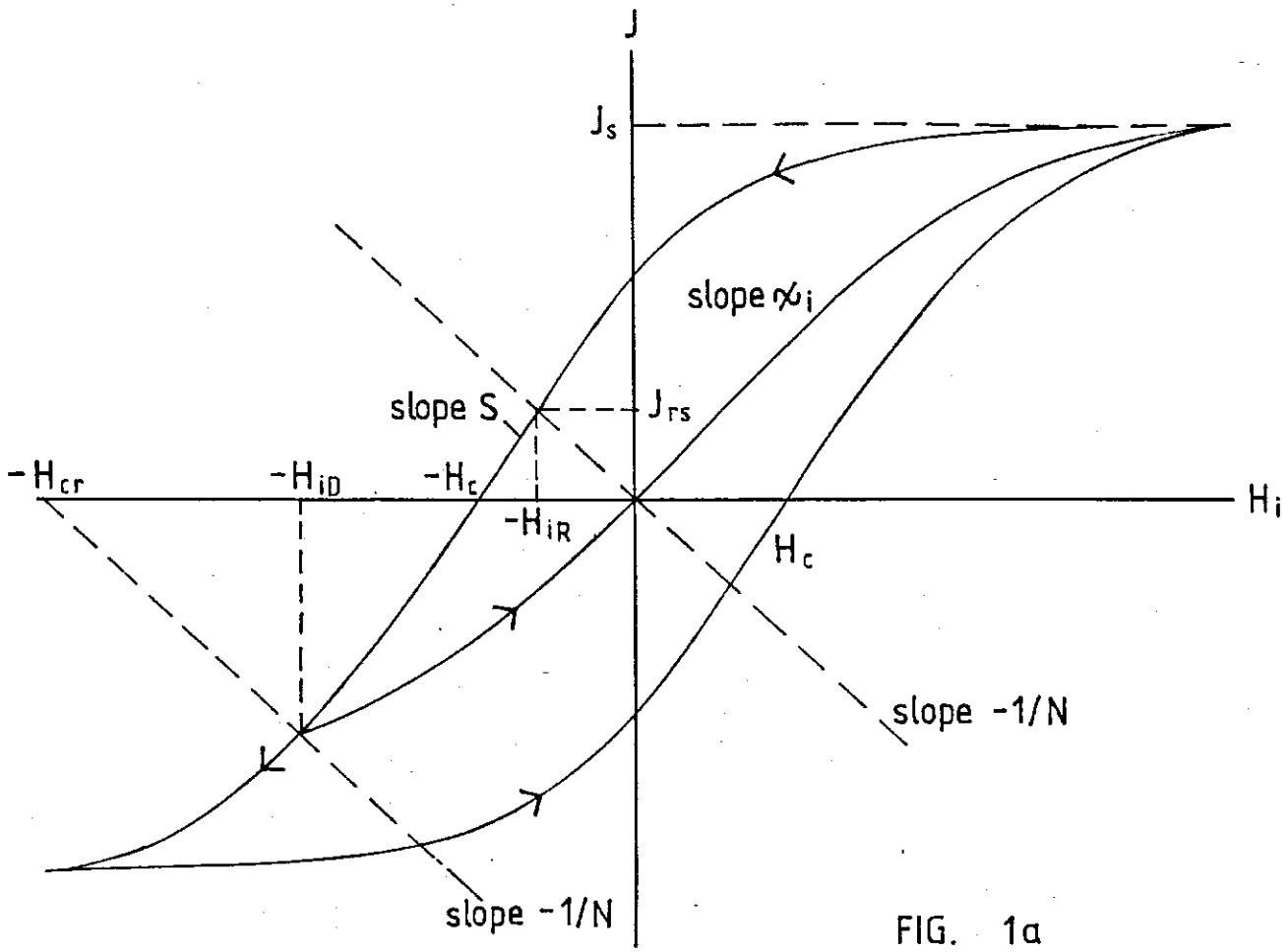
J
J_s
slope χ_i
slope S
J_{rs}
$-H_{cr}$
$-H_{iD}$
$-H_c$
$-H_{iR}$
H_i
H_c
slope -1/N
slope -1/N

FIG. 1a

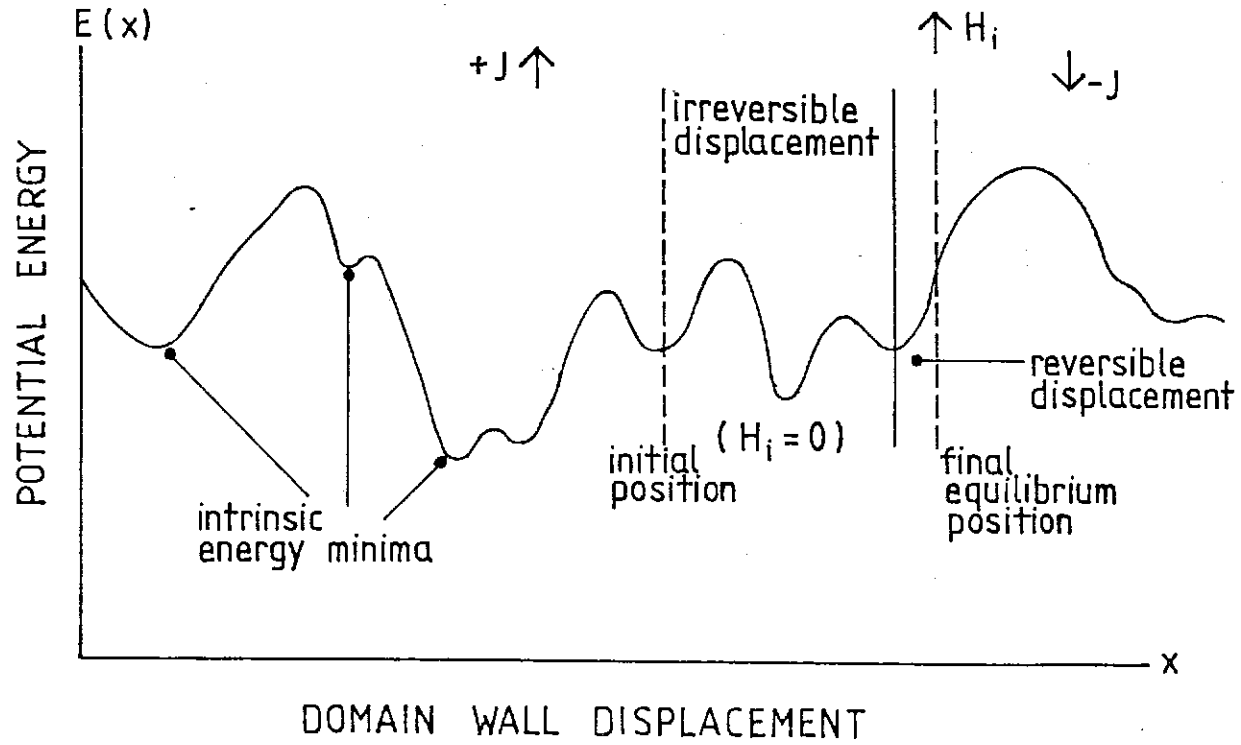
E(x)
+J
H_i
-J
irreversible displacement
POTENTIAL ENERGY
reversible displacement
$(H_i = 0)$
initial position
final equilibrium position
intrinsic energy minima
x
DOMAIN WALL DISPLACEMENT

FIG. 1b

Fig. 2(a) External hysteresis loops for multi-domain pyrrhotite grains with the applied field H_e in the basal plane ($\theta = 90^o$) and oblique to the basal plane ($\theta < 90^o$).

2(b) Idealised depiction of AF demagnetisation of saturation remanence. The grain initially descends the left-hand branch of the saturation hysteresis loop, the magnetisation decreasing from J_{rs} to J_1, and then traverses the minor hysteresis loop with average slope χ. As the amplitude of the alternating applied field is decreased to zero, smaller minor hysteresis loops are traversed (not shown) until the magnetisation of the grain converges onto the centre of the minor loop, which lies on the line of slope $-1/N$ through the origin.

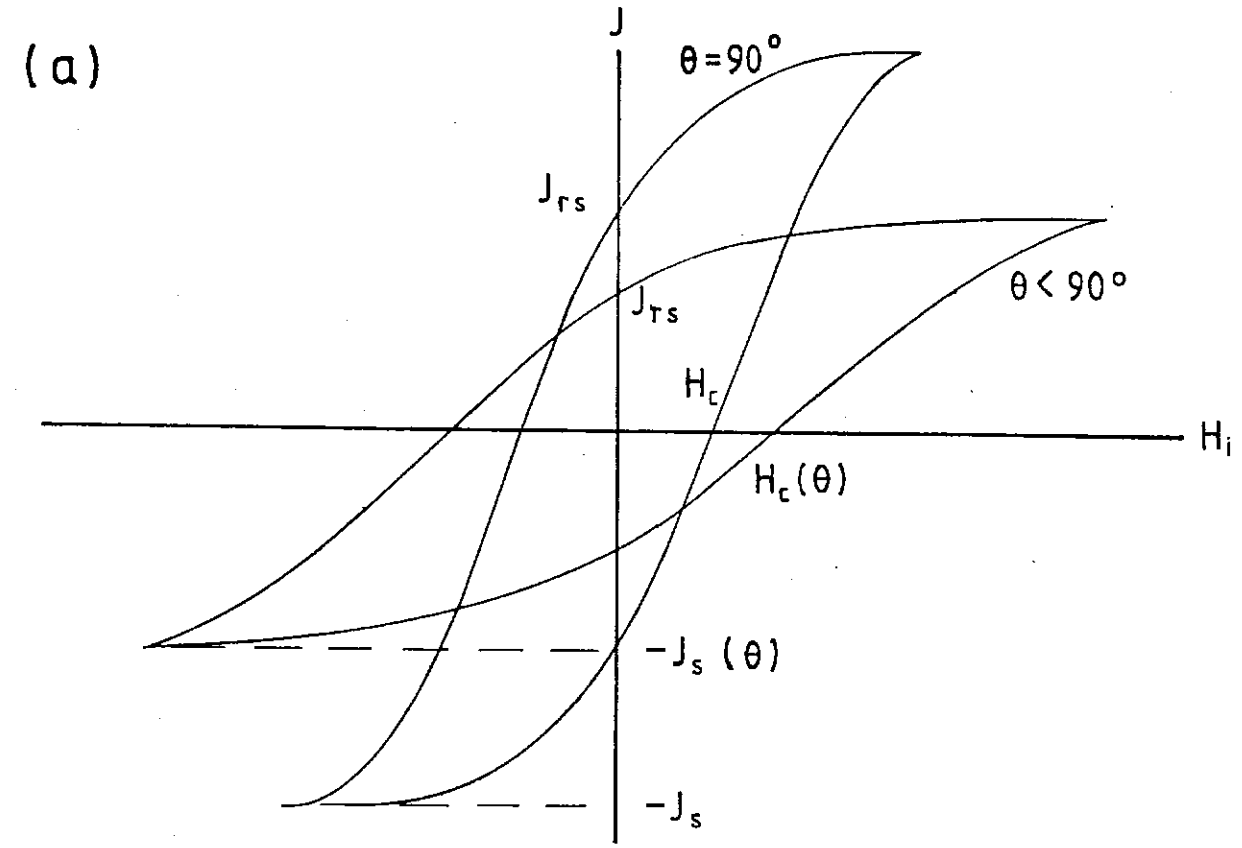
(a)
J
θ=90°
J_{rs}
J_{rs}
θ < 90°
H_c
H_i
$H_c(\theta)$
$-J_s(\theta)$
$-J_s$

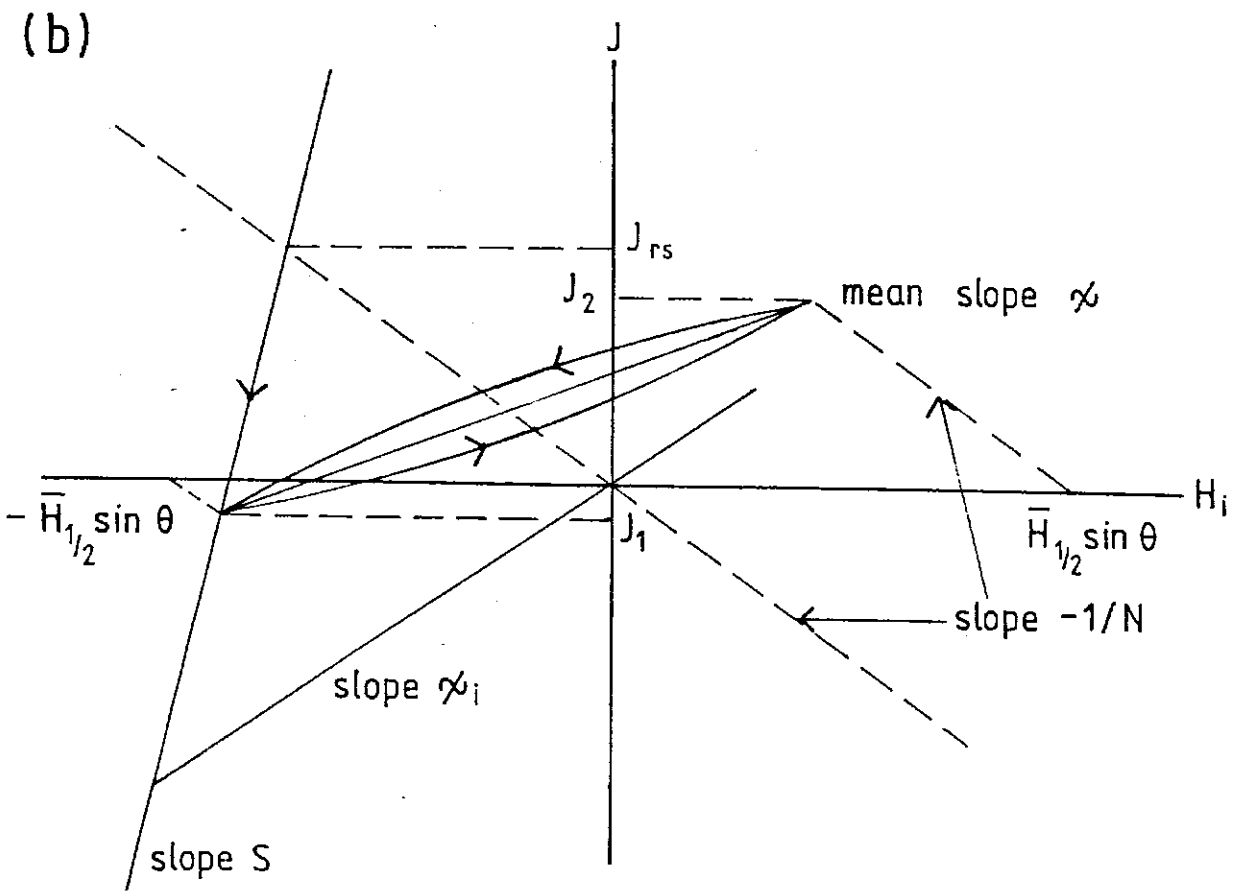
(b)
J
J_{rs}
J_2
mean slope χ
H_i
$-\bar{H}_{1/2}\sin\theta$
J_1
$\bar{H}_{1/2}\sin\theta$
slope -1/N
slope χ_i
slope S

FIG. 2

Fig. 3 Thermal activation nomogram for monclinic pyrrhotite. The contours join time-temperature conditions of equal probability of thermally activating a magnetic grain. The B field represents the region where time is relatively effective in resetting a rapidly acquired remanent magnetisation acquired at considerably higher temperature, whereas in the A field a magnetisation is unblocked only at temperatures approaching those in which the remanence was acquired. Conversely a remanent magnetisation corresponding to the B field which was acquired over a geologically long time (a viscous PTRM) will only be unblocked in the laboratory at a temperature well above the temperature of acquisition. In the A region the temperature of acquisition and the laboratory unblocking temperature are similar, irrespective of the duration of acquisition. The dashed lines enclose the region within which monoclinic 4C pyrrhotite is unstable with respect to 1C pyrrhotite + pyrite, precluding acquisition of remanence.

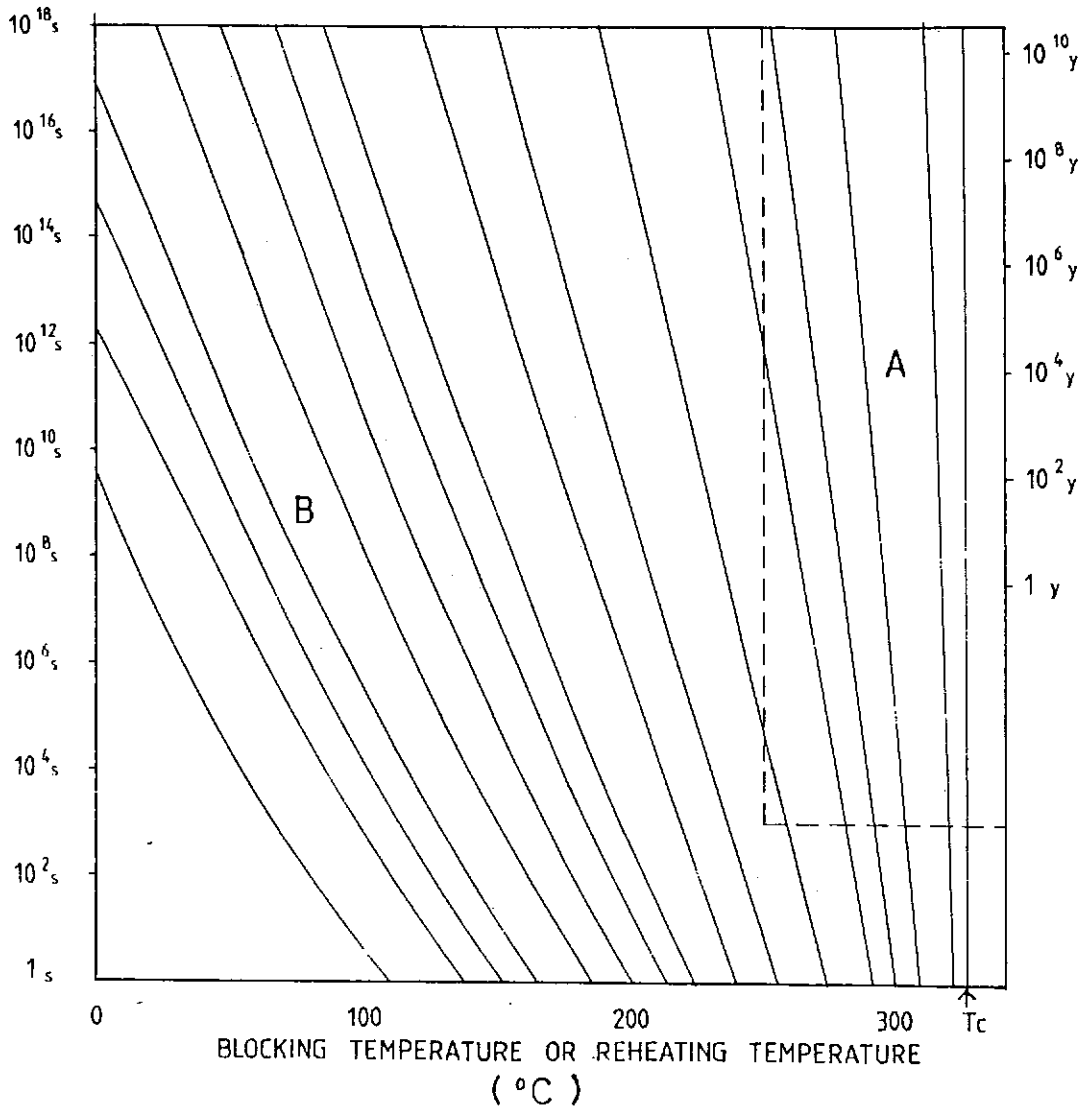

THERMAL ACTIVATION NOMOGRAM FOR MONOCLINIC PYRRHOTITE

FIG. 3